

# Beyond Semantic to Instance Segmentation: Weakly-Supervised Instance Segmentation via Semantic Knowledge Transfer and Self-Refinement

Beomyoung Kim<sup>1</sup> YoonJoon Yoo<sup>1,2</sup> Chaeun Rhee<sup>3</sup> Junmo Kim<sup>4</sup>

<sup>1</sup> NAVER CLOVA <sup>2</sup> NAVER AI Lab <sup>3</sup> Inha University <sup>4</sup> KAIST

## Abstract

Recent weakly-supervised semantic segmentation (WSSS) has made remarkable progress due to class-wise localization techniques using image-level labels. Meanwhile, weakly-supervised instance segmentation (WSIS) is a more challenging task because instance-wise localization using only image-level labels is quite difficult. Consequently, most WSIS approaches exploit off-the-shelf proposal technique that requires pre-training with high-level labels, deviating a fully image-level supervised setting. Moreover, we focus on *semantic drift problem*, i.e., missing instances in pseudo instance labels are categorized as background class, occurring confusion between background and instance in training. To this end, we propose a novel approach that consists of two innovative components. First, we design a *semantic knowledge transfer* to obtain pseudo instance labels by transferring the knowledge of WSSS to WSIS while eliminating the need for off-the-shelf proposals. Second, we propose a *self-refinement* method that refines the pseudo instance labels in a self-supervised scheme and employs them to the training in an online manner while resolving the semantic drift problem. The extensive experiments demonstrate the effectiveness of our approach, and we outperform existing works on *PASCAL VOC2012* without any off-the-shelf proposal techniques. Furthermore, our approach can be easily applied to the point-supervised setting, boosting the performance with an economical annotation cost. The code will be available soon.

## Introduction

Weakly-supervised image segmentation has actively been studied to reduce the expensive annotation cost by utilizing weak supervision such as image-level labels (Ahn, Cho, and Kwak 2019) and points (Bearman et al. 2016). Most existing weakly-supervised semantic segmentation (WSSS) approaches (Wei et al. 2017; Huang et al. 2018) exploit class activation maps (CAMs) (Zhou et al. 2016) to obtain class-wise localization maps using image-level labels, and recent studies (Kim, Han, and Kim 2021; Lee et al. 2021b) have achieved a remarkable performance comparable to the full supervision. Contrary to the success of the WSSS, weakly-supervised instance segmentation (WSIS) using image-level labels is still yet an open task because the CAM has a limitation in obtaining instance-wise localization maps.

To deal with the challenges of WSIS, most previous approaches (Zhou et al. 2018; Arun, Jawahar, and Kumar

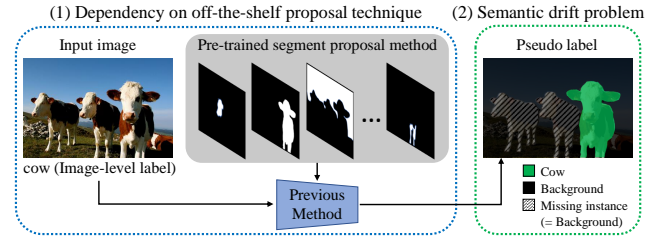


Figure 1: Two limitations of previous WSIS method: (1) dependency on off-the-shelf proposal technique that requires pre-training with high-level labels; (2) semantic drift problem between background and instance because missing instances in the pseudo label are guided as background class.

2020) utilize off-the-shelf proposal techniques. Specifically, they vote for suitable instance masks from segment proposals generated by MCG (Pont-Tuset et al. 2016) and generate pseudo instance labels to train the network. However, they have two limitations as illustrated in Figure 1. (1) Their dependency on the off-the-shelf proposal technique is considerably high, and the proposal technique requires pre-training with object boundary labels, deviating a fully image-level supervised setting. (2) Noisy pseudo labels containing missing instances can incur the semantic drift problem. As shown in Figure 1, the left two missing cows are guided to the background class and the right cow is guided to the cow class, although all cows have semantically similar visual cues. This semantic drift between background and instance confuses the network and deteriorates the stable training convergence.

In this paper, we propose a novel WSIS approach consisting of two innovative components: *semantic knowledge transfer* and *self-refinement*. Specifically, we take the advantage of the success of the WSSS method and transfer the knowledge of WSSS to WSIS, and this process is named *semantic knowledge transfer*. Using the knowledge of WSSS and instance cues, we generate rough pseudo instance labels. Here, to obtain the instance cues from image-level labels, we propose a *peak attention module (PAM)* that makes the CAM highlight the sparse representative region of objects. As a result, only image-level labels are involved in our approach including the WSSS, eliminating the proposal technique.

However, when training only with the pseudo instance labels generated from the *semantic knowledge transfer*, the

semantic drift problem follows because numerous missing instances (*i.e.*, false-negatives) in the pseudo labels can incur semantic drift between background and instance. To address the semantic drift problem, we introduce an *instance-aware guidance* strategy that dynamically assigns the guidance region only to the labeled instance region. This strategy allows the network to stably train and progressively capture instance-level information about the missing instances. Along with this strategy, to further refine the pseudo labels, we propose the self-supervised instance label refinement method that converts false-negatives to true-positives in a self-supervised manner and reflects them back to the training in an online manner. This method, shortly named *self-refinement*, improves the quality of the pseudo labels as training progresses.

The extensive experiments on PASCAL VOC 2012 (Everingham et al. 2010) show the effectiveness of the proposed design. Our method achieves a state-of-the-art performance of 51.0%  $mAP_{50}$  even without the off-the-shelf proposal techniques. Furthermore, we model the point-supervised instance segmentation by replacing the instance cues with point labels and can further boost the performance to 56.0%  $mAP_{50}$  with an economical annotation cost.

Our contribution can be summarized as follows:

- We propose a novel WSIS approach that is a fully image-level supervised setting without the proposal technique pre-trained with high-level labels and resolves the *semantic drift* problem that has not been considered so far.
- We design the *semantic knowledge transfer* strategy to obtain pseudo instance labels by transferring the knowledge of WSSS and instance cues extracted from the proposed PAM to WSIS while eliminating the use of off-the-shelf proposal techniques.
- We propose a *self-refinement* method to refine the pseudo instance labels in a self-supervised manner and reflect them back to the training in an online manner. Here, we introduce the *instance-aware guidance* strategy to resolve the semantic drift problem.

## Related Work

### Weakly-supervised semantic segmentation (WSSS)

Most WSSS studies adopting image-level labels exploit CAMs (Zhou et al. 2016) to localize class-wise object regions. However, CAMs mainly focus on the sparse discriminative object regions, resulting in low-quality pseudo segmentation labels. To address this issue, recent WSSS approaches have proposed a method to expand activation regions. AE-PSL (Wei et al. 2017) erases discriminative object regions, shifting attention to adjacent non-discriminative regions. DSRG (Huang et al. 2018) introduced a seeded region growing method to enlarge activation regions. DRS (Kim, Han, and Kim 2021) proposed a module that suppresses discriminative regions to expand activation regions. However, these approaches exploited the off-the-shelf guidance, *i.e.*, saliency map. To eliminate the dependency on the saliency map, some approaches have proposed a saliency map-free method: RRM (Zhang et al. 2020) designed an end-to-

end network to jointly produce both CAMs and segmentation output and generated pseudo labels from only reliable pixels; SingleStage (Araslanov and Roth 2020) designed a single-stage network and proposed pixel-adaptive mask refinement for self-supervised segmentation learning.

### Instance Segmentation

Unlike semantic segmentation categorizing the pixel region in class-level, instance segmentation requires an instance-level mask. The most widely used approach is a box-based two-stage method, *e.g.*, Mask R-CNN (He et al. 2017), that predicts bounding boxes and then extracts the instance mask for each bounding box; this approach has reigned on the throne with state-of-the-art performance. Recently, for the simple instance segmentation process, box-free one-stage instance segmentation methods (Neven et al. 2019; Cheng et al. 2020) have been proposed. They represent each instance using 2-dimensional (2D) offset vectors; the pixels covering each instance are represented as 2D offset vectors directed to the center of each instance. The center point of each instance is extracted from the center heatmap (Cheng et al. 2020) or by clustering 2D offset vectors (Neven et al. 2019) and the instance mask is obtained from instance grouping with the center point and 2D offset vectors.

### Weakly-supervised instance segmentation (WSIS)

WSIS is more challenging than WSSS because it is difficult to obtain instance-level information from image-level labels. This difficulty makes the recent studies exploit the off-the-shelf guidances. PRM (Zhou et al. 2018) extracts the peak point of each instance from CAMs and obtains the peak response map through peak back-propagation. Then, utilizing the response map, they select appropriate segment proposals generated by MCG (Pont-Tuset et al. 2016). To produce the dense peak response map, IAM (Zhu et al. 2019) proposes an instance extent filling module. Arun et al. (Arun, Jawahar, and Kumar 2020) modeled the uncertainty in the pseudo label generation process and iteratively trained the network using the pseudo labels. However, the MCG requires pre-training with high-level supervision, class-agnostic object boundary. Some approaches (Ge et al. 2019; Hwang et al. 2021) adopt the box-based two-stage approach and exploit a box proposal technique, selective search (Uijlings et al. 2013). These methods perform the RoI pooling (Girshick 2015) on the proposed boxes and infer the instance mask within each box region using CAMs. IRN (Ahn, Cho, and Kwak 2019) proposed a novel proposal-free method that exploits class-equivalence relations between a pair of pixels and represents instance-level information using their displacement field. However, they have trouble in obtaining accurate instance-level information because their inter-pixel relations are based on inter-class, not inter-instance, and their displacement field suffers from the semantic drift problem. To the best of our knowledge, existing methods have not yet considered the semantic drift problem caused by missing instances in their pseudo labels, which is one of the fundamental challenges that should be addressed for WSIS.

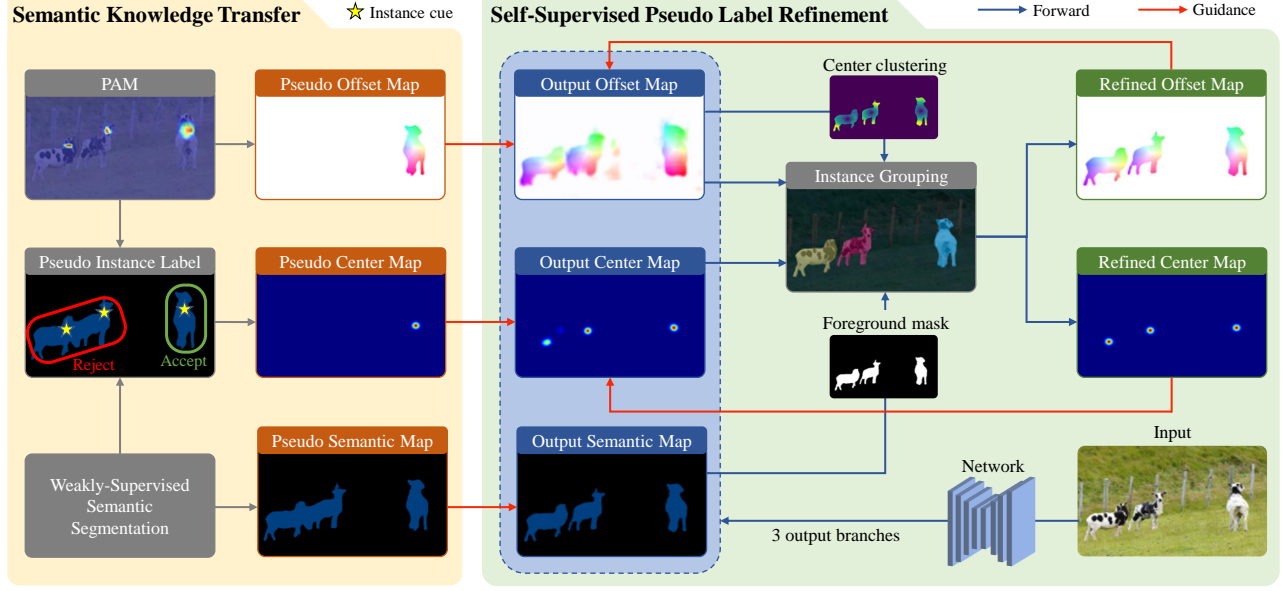


Figure 2: The overview of our framework consisting two-innovated steps: *semantic knowledge transfer* and *self-refinement*. In the *semantic knowledge transfer*, we obtain pseudo instance labels by utilizing the knowledge of WSSS and instance cues. Here, we obtain instance cues using the proposed *peak attention module (PAM)*. In the *self-refinement*, the network refines the pseudo labels in a self-supervised scheme and reflects them to the training in an online manner. For the stable training with alleviating the semantic drift problem, we apply the proposed *instance-aware guidance* strategy. Note that we exploit only the image-level labels as our supervision source with taking away the off-the-shelf guidance.

## Proposed Method

### Overview

First, as described in the left part of Figure 2, we obtain pseudo instance labels utilizing the knowledge of WSSS and instance cues, and this process is called *semantic knowledge transfer*. Here, we extract instance cues from image-level labels using the proposed *peak attention module (PAM)* module. Then, we apply the *self-supervised pseudo label refinement* strategy that refines the pseudo instance labels in a self-supervised scheme and reflects them to the training in an online manner as described in the right part of Figure 2. In order to resolve the semantic drift problem and ensure stable training, we introduce the *instance-aware guidance* strategy. Note that we employ only the image-level labels as our guidance source in our framework including the WSSS part, taking away any off-the-shelf proposal techniques.

### Preliminary: Instance Representation

Motivated by Panoptic-DeepLab (Cheng et al. 2020), we represent an instance as a center point and corresponding 2D offset vectors; the 2D offset vectors direct the center point of each instance. By adopting this representation method, we construct an instance segmentation network following the architecture of Panoptic-DeepLab, which consists of three output branches: semantic segmentation map, center map, and offset map. For the post-processing, we extract center points of each instance from the center map; pixel locations with the same value before and after the max-pooling of the center map are regarded as center points. Then, we allocate the ID of each instance in a pixel-level, and this procedure is

called as instance grouping; when the extracted  $n$ -th center point is denoted as  $(x_n, y_n)$  and the offset map is denoted as  $\mathcal{O}(i, j)$  at the pixel location  $(i, j)$ , the instance ID  $k_{i,j}$  at the pixel  $(i, j)$  becomes

$$k_{i,j} = \underset{k}{\operatorname{argmin}} ||(x_k, y_k) - ((i, j) + \mathcal{O}(i, j))||. \quad (1)$$

Note that the semantic segmentation map provides the foreground region, and the instance grouping is performed within the provided foreground region.

### Semantic Knowledge Transfer

The recent WSSS methods using only image-level labels have shown comparable performance to the full supervision. For the effective WSIS using image-level labels without the off-the-shelf proposal techniques, we propose a novel strategy, named **semantic knowledge transfer**, that transfers the knowledge of well-studied WSSS to WSIS. To begin with, we rethink the conditions of semantic and instance segmentation. The *first condition* is that instance segmentation should separate overlapping instances of the same class, unlike semantic segmentation. And the *second condition* is that semantic segmentation and instance segmentation are equivalent to each other when instances of the same class do not overlap. Based on these conditions, we design the strategy to generate pseudo instance labels using the knowledge of WSSS. From the WSSS output, we check whether instances overlap or not using instance presence cues. Then, we select a non-overlapping instance mask as a pseudo instance mask as described in the left part of Figure 2. Specifically,



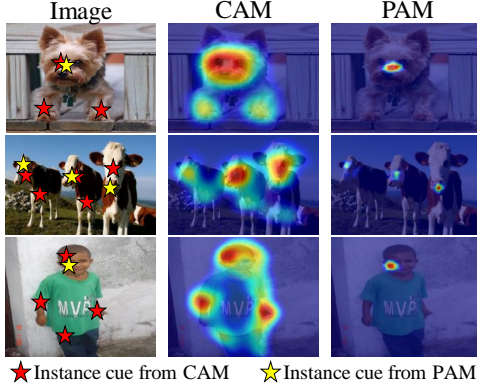


Figure 3: The activation maps from CAM and PAM. PAM helps extract more accurate instance cues than CAM.

by performing the connected component labeling (CCL) algorithm (He et al. 2009) on the WSSS output of each class, we obtain instance mask candidates and check how many instance cues are in each instance mask candidate. Following the *second condition*, the instance mask candidate with only one instance cue is adopted as the pseudo instance mask.

For the proper *semantic knowledge transfer*, we require the accurate instance cue extraction method using only image-level labels. The previous work, PRM (Zhou et al. 2018), extracts the instance cue from CAMs (Zhou et al. 2016). However, CAMs have a limitation in obtaining the accurate instance cue because several instance cues might be extracted in a single instance due to noisy activation regions as illustrated in Figure 3; it disturbs the generation of pseudo instance labels by not satisfying the *second condition*. To address this limitation, we propose a **peak attention module (PAM)** to extract accurate instance cue per instance, motivated by DRS (Kim, Han, and Kim 2021). DRS suppresses discriminative object regions, spreading attention to adjacent non-discriminative regions in a self-supervised manner. Contrary to the DRS, our PAM aims to strengthen the attention on peak (discriminative) regions, while weakening the attention on noisy activation regions. PAM consists of three parts, as illustrated in Figure 4: *selector*, *controller*, and *peak stimulator*. We denote the intermediate feature map as  $X \in \mathbb{R}^{H \times W \times C}$ , where  $H$ ,  $W$ , and  $C$  are the height, width, and the number of channels of  $X$ , respectively. The *selector* selects criteria points of peak regions using the global max pooling of  $X$ , and the criteria points are denoted as  $S_p \in \mathbb{R}^{1 \times 1 \times K}$ . The *controller* adaptively determines how much strengthen the attention on peak regions and the output of the *controller*,  $G_p \in [0, 1]^{1 \times 1 \times K}$ , is:

$$G_p = \sigma(f(GAP(X); \theta_p)), \quad (2)$$

where  $\sigma$  is a sigmoid function,  $GAP$  is a global average pooling,  $f$  is a fully connected layer, and  $\theta_p$  is learnable parameters of the *controller*. We strengthen the attention on peak regions by deactivating the attention on noisy regions. In particular,  $\tau_p = S_p \cdot G_p$  plays a role of the boundary of peak regions where  $\cdot$  is an element-wise multiplication. The regions in  $X$  higher than  $\tau_p$  are regarded as peak regions, otherwise regarded as noisy regions. We deactivate the noisy

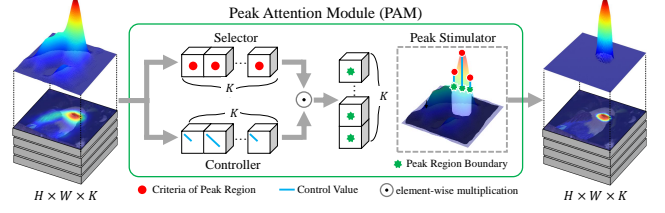


Figure 4: PAM architecture. From the selector, criteria of peak regions are selected. For a better explanation, three of them are illustrated in red points. Then, the controller determines how much to strengthen the attention on peak regions with control values, and each value is illustrated as the length of a blue line. Using criteria points and control values, the boundary of peak regions is set, and the stimulator strengthens the attention on peak regions by deactivating noisy regions whose values are lower than the boundary.

regions by setting the value to zero, increasing the attention on peak regions. The PAM is plugged into the classifier, and we produce activation maps that localize the sparse representative region of each object as shown in Figure 3 and then extract peak points (instance cues) whose values are higher than  $\delta_p$ ;  $\delta_p$  is set to 0.5. Note that the  $\theta_p$  is optimized with the objective function of the classifier, and our PAM is trained with a self-supervised manner to adaptively focus on peak regions while increasing classification ability.

Combined with the knowledge of WSSS and instance cues extracted from our PAM, we can obtain pseudo instance masks and convert these masks into the pseudo center and offset maps following our instance representation method, as illustrated in Figure 2. For the center map, the centroid point of each pseudo instance mask is encoded in a 2D Gaussian kernel with a standard deviation of 8 pixels. For the offset map, all pixels in the pseudo instance mask contain 2D offset vectors directed to the corresponding center point.

## Instance-aware Guidance

When training only with the pseudo instance labels obtained by the *semantic knowledge transfer*, we should handle the semantic drift problem. Since the missing instances in the pseudo labels are guided as a background class, semantic drift between background and instance deteriorates the stable training convergence. For example, as shown in Figure 2, the two cows on the left (*i.e.*, missing instances) are guided as a background, however, one cow on the right (*i.e.*, labeled instance) is guided as a cow; it confuses the network, and we define this problem as the semantic drift. To alleviate this problem, we introduce an **instance-aware guidance** by taking the advantage of our instance representation method. The semantic segmentation map determines the foreground region, and the offset and center maps play an essential role in representing instance-level information within the foreground region. In other words, the background region of the offset and center maps can be regarded as ignoring regions in both training and inference. Therefore, we assign the guidance region for the offset and center maps to only the region for the labeled instances; this strategy is called the *instance-*

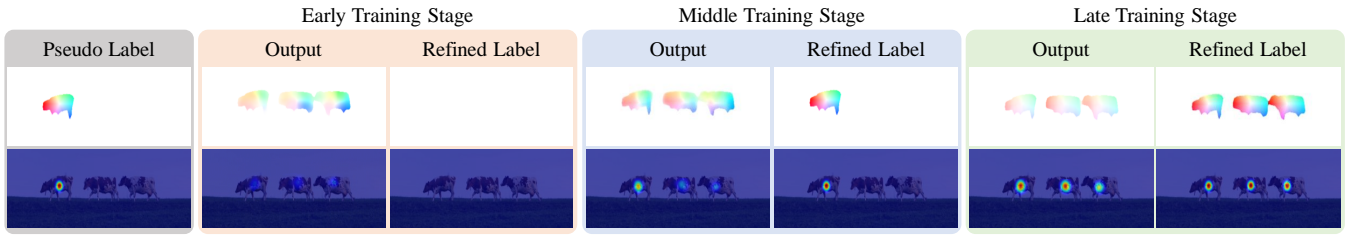


Figure 5: Comparison of offset and center maps. As training progresses, the network generates the high-quality refined label.

*aware guidance* and helps alleviate the semantic drift problem because the region of the offset and center maps for the missing instances (*e.g.*, the white region of the pseudo offset map in Figure 2) is not reflected in the objective function. Consequently, as shown in Figure 5, the network can stably capture the instance-level information of the missing instances as the training progresses.

### Self-Supervised Pseudo Label Refinement

Even we can alleviate the semantic drift problem, the number of true-positives in the pseudo labels is still not enough (about 30% true-positives in the pseudo labels) for training the network. Here, we propose a self-supervised pseudo label refinement strategy that refines the pseudo labels by converting false-negatives to true-positives in a self-supervised manner and reflects the refined labels to the training in an online manner. We shortly name this strategy as **self-refinement**. The overall process of the *self-refinement* is illustrated on the right side of Figure 2. First, by training with the pseudo instance labels using the *instance-aware guidance* strategy, the network stably develops the generalization ability and gradually captures the instance-level information of the missing instances (*i.e.*, false-negatives). Next, following the Eq. (1), we perform the instance grouping using the network outputs. Then, we generate refined offset and center maps from the instance mask created by instance grouping. Last, the refined maps are used as guidance for the network.

For better refinement, we maximize the complementary knowledge between each network output. Specifically, the noisy output offset map can be transformed into the refined offset map containing 2D offset vectors with exact values by grouping with the output center map. Likewise, we can complement the output center map using the knowledge of the output offset map. We cluster the center point from the output offset map utilizing the fact that 2D offset vectors near the center point have a small magnitude value; we call this process a **center clustering** and explain the detailed algorithm in the supplementary material. The clustered center points help to generate the refined center map by filling the missing centers in the output center map. Through the complementary knowledge between each output, we upgrade the pseudo label refinement process to be more effective.

Using both pseudo labels and refined labels, we jointly train the network. Here, we denote the network output semantic segmentation, offset map, and center map as  $\mathcal{S}(\cdot)$ ,  $\mathcal{O}(\cdot)$ , and  $\mathcal{C}(\cdot)$ , respectively. For the *instance-aware guidance* of the offset and center maps, we collect sets of pixels for labeled instance regions from pseudo labels and refined

labels, and each set is denoted as  $\mathcal{P}_{pseudo}$  and  $\mathcal{P}_{refined}$ . To utilize the refined labels as soft labels, we design a weight mask  $\mathcal{W}(i, j)$ :

$$\mathcal{W}^n(i, j) = \begin{cases} \mathcal{C}(x_n, y_n) & (i, j) \in \mathcal{P}_{pseudo}^n, \\ 0 & \text{otherwise,} \end{cases} \quad (3)$$

where the center point of  $n$ -th instance in the refined labels are denoted as  $(x_n, y_n)$ , and  $\mathcal{C}(x_n, y_n)$  means the confidence score of the  $n$ -th instance. The  $\mathcal{W}$  is exploited as the weight of the objective function for the refined labels. The objective function of the center map is defined as:

$$\mathcal{L}_{center} = \frac{1}{|\mathcal{P}_{pseudo}|} \sum_{(i,j) \in \mathcal{P}_{pseudo}} (\mathcal{C}(i, j) - \hat{\mathcal{C}}(i, j))^2 + \frac{1}{|\mathcal{P}_{refined}|} \sum_{(i,j) \in \mathcal{P}_{refined}} \mathcal{W}(i, j) \cdot (\mathcal{C}(i, j) - \bar{\mathcal{C}}(i, j))^2, \quad (4)$$

where the pseudo and refined center maps are  $\hat{\mathcal{C}}(i, j)$  and  $\bar{\mathcal{C}}(i, j)$ , respectively. Also, the objective function of the offset map is defined as:

$$\mathcal{L}_{offset} = \frac{1}{|\mathcal{P}_{pseudo}|} \sum_{(i,j) \in \mathcal{P}_{pseudo}} |\mathcal{O}(i, j) - \hat{\mathcal{O}}(i, j)| + \frac{1}{|\mathcal{P}_{refined}|} \sum_{(i,j) \in \mathcal{P}_{refined}} \mathcal{W}(i, j) \cdot |\mathcal{O}(i, j) - \bar{\mathcal{O}}(i, j)|, \quad (5)$$

where the pseudo and refined offset maps are  $\hat{\mathcal{O}}(i, j)$  and  $\bar{\mathcal{O}}(i, j)$ , respectively. Lastly, the objective function of the segmentation map is defined as:

$$\mathcal{L}_{sem} = -\frac{1}{|\mathcal{P}_{sem}|} \sum_{(i,j) \in \mathcal{P}_{sem}} \log \mathcal{S}(i, j), \quad (6)$$

where  $\mathcal{S}$  is the output semantic map and  $\mathcal{P}_{sem}$  is the set of all pixels in  $\mathcal{S}$ . The network is jointly trained with the above three objective functions, and the final objective function is:

$$\mathcal{L} = \lambda_{center} \mathcal{L}_{center} + \lambda_{offset} \mathcal{L}_{offset} + \lambda_{sem} \mathcal{L}_{sem}, \quad (7)$$

where  $\lambda$  is a weight parameter, and empirically set  $\lambda_{center} = 200$ ,  $\lambda_{offset} = 0.01$ , and  $\lambda_{sem} = 20$ .

Through our *self-refinement* strategy, the pseudo labels can convert into high-quality refined labels. The refined labels are generated from the network in an online manner at every mini-batch. Also, since most of the processes are performed by GPU operation, the latency of the *self-refinement* is negligibly small.

PAM	IAG	refine	cluster	$mAP_{50}$
✗	✗	✗	✗	12.3
✓	✗	✗	✗	28.8
✓	✓	✗	✗	38.6
✓	✓	✓	✗	40.8
✓	✓	✓	✓	41.1

Table 1: Effect of the proposed methods: PAM, IAG (*instance-aware guidance*), refine (*self-refinement*), and cluster (*center clustering*).

Table 2: Analysis of the effect of WSSS result on our WSIS performance. We measure the  $mAP_{50}$  instance segmentation performance according to WSSS methods.

Semantic Segmentation		Instance Segmentation
WSSS method	mIoU	$mAP_{50}$
SingleStage (Araslanov and Roth 2020)	62.7	39.7
SSDD (Shimoda and Yanai 2019)	64.9	40.7
RRM (Zhang et al. 2020)	66.3	41.1
DRS (Kim, Han, and Kim 2021)	70.4	42.0
ground truth	-	49.4

## Experiments

### Dataset and Evaluation Metrics

We demonstrate the effectiveness of the proposed approach on PASCAL VOC 2012 dataset (Everingham et al. 2010), which contains 1464 training, 1449 validation, and 1456 testing images with 20 object categories. Following the common practice in previous works, the training set is augmented to 10,582 images. We evaluate the performance using the mean average precision (mAP) with intersection-over-union (IoU) thresholds of 0.25, 0.5, 0.7, and 0.75.

### Implementation Details

For the *semantic knowledge transfer*, we extract instance cues from the classifier equipped with our PAM. We describe the detailed architecture of the classifier and analysis in the supplementary material. For the WSSS method, we adopt RRM (Zhang et al. 2020) that requires only the image-level supervision without saliency maps, therefore, we can keep a fully extra guidance-free setting.

For the instance segmentation network, we follow the network structure of Panoptic-DeepLab (Cheng et al. 2020) with a modification; we change the center map from class-agnostic to class-wise for more accurate instance grouping. The backbone network is ResNet-50 (He et al. 2016) pre-trained on ImageNet (Deng et al. 2009). We train the network for the 60K iterations with 16 batch size using Adam optimizer (Kingma and Ba 2014) with a 0.0001 initial learning rate and the polynomial learning rate decay scheduling (Liu, Rabinovich, and Berg 2015). Some approaches (Ahn, Cho, and Kwak 2019; Liu et al. 2020) adopt an additional training step on Mask R-CNN. We denote this step as Mask R-CNN refinement, and for a fair comparison, we apply this step using pseudo labels generated from our network, strictly following the Mask R-CNN training settings.

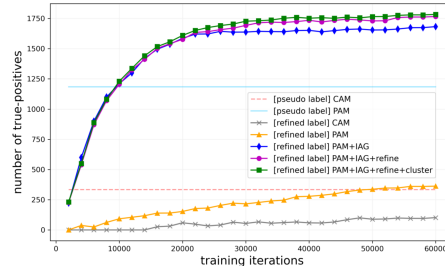


Figure 6: Evolution of the number of true-positives on VOC 2012 train set.

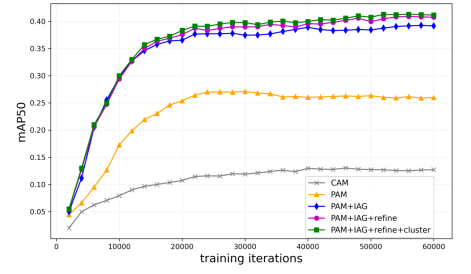


Figure 7: Evolution of the  $mAP_{50}$  on VOC 2012 validation set.

### Analysis

For analysis, we skip the Mask R-CNN refinement step and follow the mentioned implementation details. We count the number of true-positives on VOC 2012 train set containing 1464 images and 3507 instances in Figure 6 and measure the  $mAP_{50}$  on VOC 2012 validation set in Figure 7.

**Effect of PAM:** We analyze the effect of the proposed PAM by comparing it with the CAM. As shown in Figure 3, we have trouble in obtaining proper instance cues from conventional CAM due to the noisy activation regions. However, with our PAM, we can extract appropriate instance cues, which tremendously helps the proper *semantic knowledge transfer* and obtain three times more true-positive training samples than the CAM as shown in Figure 6, giving a 16.5% improvement as in the first and second rows of Table 1.

**Effect of Instance-aware Guidance:** For analysis, we train the network without IAG (*instance-aware guidance*), that is, the whole region (including background region) of the offset and center maps are reflected in the objective function. As in the first and third rows of Table 1, without IAG, the performance drops by 9.8% because it suffers from the semantic drift problem as mentioned in the method section. Also, as shown in Figure 7, the model without IAG seems to be stuck in a local minimum, whereas the model with IAG seems to avoid the local minimum, enhancing the performance as training progresses. This result convinces us that IAG is effective to alleviate the semantic drift problem.

**Effect of Self-Refinement:** For analysis, we compare the result of the network trained only pseudo labels without the *self-refinement*. As shown in Figure 6, the increase in the number of true-positives proves that we can obtain the high-quality refined labels as training progresses. Since the refined labels are guided to the training, the network can further enhance the self-refinement ability; this progressive self-refinement yields a 2.2% improvement.

**Effect of Center Clustering:** In the first and last rows of Table 1, we analyze the effect of the center clustering. Without the center clustering, the performance drops by 0.3%. This result demonstrates that the center clustering can enhance complementary knowledge between each network output.

**Influence of WSSS method:** In Table 2, we analyze how the WSSS result affects the WSIS. Originally, we adopt RRM (Zhang et al. 2020) for our WSSS method, which shows 66.3% mIoU on VOC 2012 validation set. When we adopt SingleStage (Araslanov and Roth 2020), which shows



Table 3: Comparison of state-of-the-art weakly-supervised instance segmentation methods on the Pascal VOC 2012 validation set. MRCNN indicates applying Mask R-CNN refinement. We denote supervision sources as:  $\mathcal{F}$  (full mask),  $\mathcal{I}$  (image-level label),  $\mathcal{P}$  (point),  $\mathcal{C}$  (object count). We indicate the annotation cost per image in seconds for each supervision source. The  $\mathcal{M}$  and  $\mathcal{R}$  denote segment proposal (MCG) and region proposal (selective search) methods, respectively.

Method	MRCNN	Sup	Extra	$mAP_{25}$	$mAP_{50}$	$mAP_{70}$	$mAP_{75}$	Cost
Mask R-CNN (He et al. 2017)	✓	$\mathcal{F}$	-	76.7	67.9	52.5	44.9	239.7
PRM (Zhang et al. 2020)	✗	$\mathcal{I}$	$\mathcal{M}$	44.3	26.8	-	9.0	20.0
IAM (Zhu et al. 2019)	✗	$\mathcal{I}$	$\mathcal{M}$	45.9	28.3	-	11.9	20.0
Label-PEnet (Ge et al. 2019)	✗	$\mathcal{I}$	$\mathcal{R}$	49.2	30.2	-	12.9	20.0
CL (Hwang et al. 2021)	✗	$\mathcal{I}$	$\mathcal{M}, \mathcal{R}$	<b>56.6</b>	38.1	-	12.3	20.0
ours	✗	$\mathcal{I}$	-	54.0	<b>41.1</b>	<b>28.0</b>	<b>23.6</b>	20.0
OCIS (Cholakkal et al. 2019)	✗	$\mathcal{C}$	$\mathcal{M}$	48.5	30.2	-	14.4	22.2
WISE-Net (Laradji et al. 2020)	✗	$\mathcal{P}$	$\mathcal{M}$	53.5	43.0	-	<b>25.9</b>	23.3
ours	✗	$\mathcal{P}$	-	<b>57.8</b>	<b>45.3</b>	<b>32.1</b>	25.0	23.3
WISE (Laradji, Vázquez, and Schmidt 2019)	✓	$\mathcal{I}$	$\mathcal{M}$	49.2	41.7	-	23.7	20.0
IRN (Ahn, Cho, and Kwak 2019)	✓	$\mathcal{I}$	-	-	46.7	23.5	-	20.0
LIID (Liu et al. 2020)	✓	$\mathcal{I}$	$\mathcal{M}$	-	48.4	-	24.9	20.0
Arun et al. (Arun, Jawahar, and Kumar 2020)	✓	$\mathcal{I}$	$\mathcal{M}$	59.7	50.9	30.2	<b>28.5</b>	20.0
ours	✓	$\mathcal{I}$	-	<b>61.1</b>	<b>51.0</b>	<b>32.0</b>	26.5	20.0
ours	✓	$\mathcal{P}$	-	<b>66.2</b>	<b>56.0</b>	<b>36.5</b>	<b>29.5</b>	23.3

a 3.5% lower mIoU,  $mAP_{50}$  drops by 1.4%. Likewise, when we adopt DRS (Kim, Han, and Kim 2021), which shows a 4.1% higher mIoU,  $mAP_{50}$  boosts by 0.9%. The result shows that the performance of WSIS is relatively robust to that of WSSS because our *self-refinement* can refine some noise in the WSSS output. Note that DRS requires saliency maps, therefore, we adopt RRM as our default WSSS method because it is an extra guidance-free approach. Additionally, we train with ground-truth semantic segmentation labels and obtain a performance gain of 8.3%  $mAP_{50}$ ; this result leaves us the opportunity that the advancement of the WSSS method can improve the performance of our approach.

**Qualitative results:** As shown in Figure 8, we properly segment overlapping instances. More qualitative samples and failure cases are provided in our supplementary material.

### Point-Supervised Instance Segmentation

In our framework, we can exploit point labels as weak labels. According to (Bearman et al. 2016; Bellver Bueno et al. 2019), annotation costs are as follow: image-level (20.0 sec/img), object count (22.2 sec/img), point (23.3 sec/img), bounding box (38.1 sec/img), full mask (239.7 sec/img). The point label is an economical label that is 16% more expensive than the image-level label. For our point-supervised setting, we replace instance cues from PAM with point labels for the *semantic knowledge transfer* and replace the pseudo and refined center maps with the ground-truth center map for the *self-refinement*. When adopting the point supervision, we can obtain 10% more true-positives in pseudo labels due to the accurate instance cue. In addition, since the network can be trained with the ground-truth center map, the network can further develop the self-refinement ability, boosting the performance by 4~5% as in Table 3.

### State-of-the-arts Comparison

We compare our approach with other state-of-the-art WSIS methods in Table 3. Given only image-level supervision,

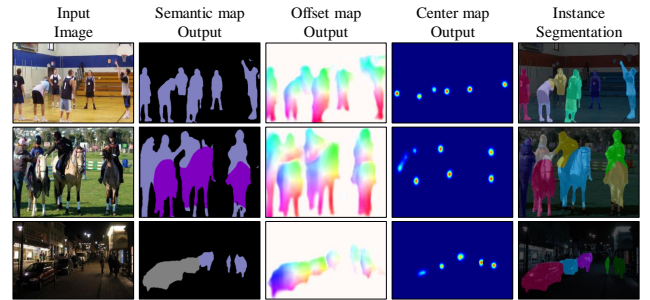


Figure 8: Qualitative results of our instance segmentation network with image-level supervision on VOC 2012 dataset.

our method outperforms existing methods even without the off-the-shelf proposal. Compared to the extra guidance-free method, IRN, our approach shows better performance (50.3% *v.s.* 46.7%) because their displacement field, which is similar to our offset map, suffer from the semantic drift problem. Given point supervision, we can further widen the performance gap with other methods at a reasonable cost.

## Conclusion

In this paper, we proposed a novel approach for WSIS by addressing the pain-points of previous methods: dependency on off-the-shelf proposals and the semantic drift problem. In our *semantic knowledge transfer*, we transferred the knowledge of WSSS combined with instance cues to WSIS and obtained pseudo instance labels. Here, to accurately extract the instance cues, we proposed the PAM module, addressing the limitations of CAMs. In our *self-refinement*, we refined the pseudo labels in a self-supervised scheme and employed them in training. For the stable learning with resolving the semantic drift problem, we introduced the *instance-aware guidance* strategy. Extensive experiments demonstrated the effectiveness of our approach, and our approach outperforms the previous methods without the off-the-shelf proposals.

## References

- Ahn, J.; Cho, S.; and Kwak, S. 2019. Weakly supervised learning of instance segmentation with inter-pixel relations. In *Proceedings of the IEEE Conference on Computer Vision and Pattern Recognition*, 2209–2218. 1, 2, 6, 7, 12, 13
- Araslanov, N.; and Roth, S. 2020. Single-stage semantic segmentation from image labels. In *Proceedings of the IEEE/CVF Conference on Computer Vision and Pattern Recognition*, 4253–4262. 2, 6
- Arun, A.; Jawahar, C.; and Kumar, M. P. 2020. Weakly supervised instance segmentation by learning annotation consistent instances. In *European Conference on Computer Vision*, 254–270. Springer. 1, 2, 7, 11
- Bearman, A.; Russakovsky, O.; Ferrari, V.; and Fei-Fei, L. 2016. What’s the point: Semantic segmentation with point supervision. In *European conference on computer vision*, 549–565. Springer. 1, 7, 11
- Bellver Bueno, M.; Salvador Aguilera, A.; Torres Viñals, J.; and Giró Nieto, X. 2019. Budget-aware semi-supervised semantic and instance segmentation. In *The IEEE Conference on Computer Vision and Pattern Recognition (CVPR) Workshops, 2019*, 93–102. 7, 11
- Cheng, B.; Collins, M. D.; Zhu, Y.; Liu, T.; Huang, T. S.; Adam, H.; and Chen, L.-C. 2020. Panoptic-deeplab: A simple, strong, and fast baseline for bottom-up panoptic segmentation. In *Proceedings of the IEEE/CVF Conference on Computer Vision and Pattern Recognition*, 12475–12485. 2, 3, 6, 11
- Cheng, B.; Parkhi, O.; and Kirillov, A. 2021. Pointly-Supervised Instance Segmentation. *arXiv preprint arXiv:2104.06404*.
- Choe, J.; Lee, S.; and Shim, H. 2020. Attention-based dropout layer for weakly supervised single object localization and semantic segmentation. *IEEE Transactions on Pattern Analysis and Machine Intelligence*.
- Cholakkal, H.; Sun, G.; Khan, F. S.; and Shao, L. 2019. Object counting and instance segmentation with image-level supervision. In *Proceedings of the IEEE conference on computer vision and pattern recognition*, 12397–12405. 7, 11
- Dai, J.; He, K.; and Sun, J. 2015. Boxsup: Exploiting bounding boxes to supervise convolutional networks for semantic segmentation. In *Proceedings of the IEEE international conference on computer vision*, 1635–1643.
- Deng, J.; Dong, W.; Socher, R.; Li, L.-J.; Li, K.; and Fei-Fei, L. 2009. Imagenet: A large-scale hierarchical image database. In *2009 IEEE conference on computer vision and pattern recognition*, 248–255. Ieee. 6
- Everingham, M.; Van Gool, L.; Williams, C. K.; Winn, J.; and Zisserman, A. 2010. The pascal visual object classes (voc) challenge. *International journal of computer vision*, 88(2): 303–338. 2, 6
- Fan, J.; Zhang, Z.; Song, C.; and Tan, T. 2020. Learning Integral Objects With Intra-Class Discriminator for Weakly-Supervised Semantic Segmentation. In *Proceedings of the IEEE/CVF Conference on Computer Vision and Pattern Recognition*, 4283–4292.
- Ge, W.; Guo, S.; Huang, W.; and Scott, M. R. 2019. Label-PEnet: Sequential Label Propagation and Enhancement Networks for Weakly Supervised Instance Segmentation. In *Proceedings of the IEEE International Conference on Computer Vision*, 3345–3354. 2, 7
- Girshick, R. 2015. Fast r-cnn. In *Proceedings of the IEEE international conference on computer vision*, 1440–1448. 2
- He, K.; Gkioxari, G.; Dollár, P.; and Girshick, R. 2017. Mask r-cnn. In *Proceedings of the IEEE international conference on computer vision*, 2961–2969. 2, 7, 11
- He, K.; Zhang, X.; Ren, S.; and Sun, J. 2016. Deep residual learning for image recognition. In *Proceedings of the IEEE conference on computer vision and pattern recognition*, 770–778. 6
- He, L.; Chao, Y.; Suzuki, K.; and Wu, K. 2009. Fast connected-component labeling. *Pattern recognition*, 42(9): 1977–1987. 4
- Hong, S.; Yeo, D.; Kwak, S.; Lee, H.; and Han, B. 2017. Weakly supervised semantic segmentation using web-crawled videos. In *Proceedings of the IEEE Conference on Computer Vision and Pattern Recognition*, 7322–7330.
- Hsu, C.-C.; Hsu, K.-J.; Tsai, C.-C.; Lin, Y.-Y.; and Chuang, Y.-Y. 2019. Weakly supervised instance segmentation using the bounding box tightness prior. *Advances in Neural Information Processing Systems*, 32: 6586–6597. 11
- Huang, Z.; Wang, X.; Wang, J.; Liu, W.; and Wang, J. 2018. Weakly-supervised semantic segmentation network with deep seeded region growing. In *Proceedings of the IEEE Conference on Computer Vision and Pattern Recognition*, 7014–7023. 1, 2
- Hwang, J.; Kim, S.; Son, J.; and Han, B. 2021. Weakly Supervised Instance Segmentation by Deep Community Learning. In *Proceedings of the IEEE/CVF Winter Conference on Applications of Computer Vision*, 1020–1029. 2, 7
- Khoreva, A.; Benenson, R.; Hosang, J.; Hein, M.; and Schiele, B. 2017. Simple does it: Weakly supervised instance and semantic segmentation. In *Proceedings of the IEEE conference on computer vision and pattern recognition*, 876–885. 11
- Kim, B.; Han, S.; and Kim, J. 2021. Discriminative Region Suppression for Weakly-Supervised Semantic Segmentation. In *Proceedings of the AAAI Conference on Artificial Intelligence*, volume 35, 1754–1761. 1, 2, 4, 6, 7
- Kingma, D. P.; and Ba, J. 2014. Adam: A method for stochastic optimization. *arXiv preprint arXiv:1412.6980*. 6
- Krähenbühl, P.; and Koltun, V. 2011. Efficient inference in fully connected crfs with gaussian edge potentials. *Advances in neural information processing systems*, 24: 109–117. 11
- Laradji, I. H.; Rostamzadeh, N.; Pinheiro, P. O.; Vazquez, D.; and Schmidt, M. 2020. Proposal-Based Instance Segmentation With Point Supervision. In *2020 IEEE International Conference on Image Processing (ICIP)*, 2126–2130. IEEE. 7, 11
- Laradji, I. H.; Vázquez, D.; and Schmidt, M. 2019. Where are the Masks: Instance Segmentation with Image-level Supervision. In *BMVC*. 7



- Lee, J.; Yi, J.; Shin, C.; and Yoon, S. 2021a. BBAM: Bounding box attribution map for weakly supervised semantic and instance segmentation. In *Proceedings of the IEEE/CVF Conference on Computer Vision and Pattern Recognition*, 2643–2652. 11
- Lee, S.; Lee, M.; Lee, J.; and Shim, H. 2021b. Railroad is not a Train: Saliency as Pseudo-pixel Supervision for Weakly Supervised Semantic Segmentation. In *Proceedings of the IEEE/CVF Conference on Computer Vision and Pattern Recognition*, 5495–5505. 1
- Li, Y.; Qi, H.; Dai, J.; Ji, X.; and Wei, Y. 2017. Fully convolutional instance-aware semantic segmentation. In *Proceedings of the IEEE conference on computer vision and pattern recognition*, 2359–2367.
- Lin, D.; Dai, J.; Jia, J.; He, K.; and Sun, J. 2016. Scribble-sup: Scribble-supervised convolutional networks for semantic segmentation. In *Proceedings of the IEEE Conference on Computer Vision and Pattern Recognition*, 3159–3167.
- Liu, W.; Rabinovich, A.; and Berg, A. C. 2015. Parzenet: Looking wider to see better. *arXiv preprint arXiv:1506.04579*. 6
- Liu, Y.; Wu, Y.-H.; Wen, P.-S.; Shi, Y.-J.; Qiu, Y.; and Cheng, M.-M. 2020. Leveraging instance-, image- and dataset-level information for weakly supervised instance segmentation. *IEEE Transactions on Pattern Analysis and Machine Intelligence*. 6, 7
- Neven, D.; Brabandere, B. D.; Proesmans, M.; and Gool, L. V. 2019. Instance segmentation by jointly optimizing spatial embeddings and clustering bandwidth. In *Proceedings of the IEEE Conference on Computer Vision and Pattern Recognition*, 8837–8845. 2
- Oh, S. J.; Benenson, R.; Khoreva, A.; Akata, Z.; Fritz, M.; and Schiele, B. 2017. Exploiting saliency for object segmentation from image level labels. In *2017 IEEE conference on computer vision and pattern recognition (CVPR)*, 5038–5047. IEEE.
- Papandreou, G.; Chen, L.-C.; Murphy, K. P.; and Yuille, A. L. 2015. Weakly-and semi-supervised learning of a deep convolutional network for semantic image segmentation. In *Proceedings of the IEEE international conference on computer vision*, 1742–1750.
- Pinheiro, P. O.; and Collobert, R. 2015. From image-level to pixel-level labeling with convolutional networks. In *Proceedings of the IEEE conference on computer vision and pattern recognition*, 1713–1721.
- Pont-Tuset, J.; Arbelaez, P.; Barron, J. T.; Marques, F.; and Malik, J. 2016. Multiscale combinatorial grouping for image segmentation and object proposal generation. *IEEE transactions on pattern analysis and machine intelligence*, 39(1): 128–140. 1, 2
- Selvaraju, R. R.; Cogswell, M.; Das, A.; Vedantam, R.; Parikh, D.; and Batra, D. 2017. Grad-cam: Visual explanations from deep networks via gradient-based localization. In *Proceedings of the IEEE international conference on computer vision*, 618–626.
- Shimoda, W.; and Yanai, K. 2019. Self-supervised difference detection for weakly-supervised semantic segmentation. In *Proceedings of the IEEE/CVF International Conference on Computer Vision*, 5208–5217. 6
- Simonyan, K.; and Zisserman, A. 2014. Very deep convolutional networks for large-scale image recognition. *arXiv preprint arXiv:1409.1556*. 10
- Tang, P.; Wang, X.; Bai, X.; and Liu, W. 2017. Multiple instance detection network with online instance classifier refinement. In *Proceedings of the IEEE Conference on Computer Vision and Pattern Recognition*, 2843–2851.
- Tian, Z.; Shen, C.; and Chen, H. 2020. Conditional convolutions for instance segmentation. In *Computer Vision—ECCV 2020: 16th European Conference, Glasgow, UK, August 23–28, 2020, Proceedings, Part I 16*, 282–298. Springer.
- Tian, Z.; Shen, C.; Wang, X.; and Chen, H. 2021. BoxInst: High-performance instance segmentation with box annotations. In *Proceedings of the IEEE/CVF Conference on Computer Vision and Pattern Recognition*, 5443–5452. 11
- Uijlings, J. R.; Van De Sande, K. E.; Gevers, T.; and Smeulders, A. W. 2013. Selective search for object recognition. *International journal of computer vision*, 104(2): 154–171. 2
- Vernaza, P.; and Chandraker, M. 2017. Learning random-walk label propagation for weakly-supervised semantic segmentation. In *Proceedings of the IEEE conference on computer vision and pattern recognition*, 7158–7166.
- Wang, X.; Zhang, R.; Kong, T.; Li, L.; and Shen, C. 2020. SOLOv2: Dynamic and Fast Instance Segmentation. *Advances in Neural Information Processing Systems*, 33.
- Wei, Y.; Feng, J.; Liang, X.; Cheng, M.-M.; Zhao, Y.; and Yan, S. 2017. Object region mining with adversarial erasing: A simple classification to semantic segmentation approach. In *Proceedings of the IEEE conference on computer vision and pattern recognition*, 1568–1576. 1, 2
- Zhang, B.; Xiao, J.; Wei, Y.; Sun, M.; and Huang, K. 2020. Reliability does matter: An end-to-end weakly supervised semantic segmentation approach. In *Proceedings of the AAAI Conference on Artificial Intelligence*, volume 34, 12765–12772. 2, 6, 7
- Zhou, B.; Khosla, A.; Lapedriza, A.; Oliva, A.; and Torralba, A. 2016. Learning deep features for discriminative localization. In *Proceedings of the IEEE conference on computer vision and pattern recognition*, 2921–2929. 1, 2, 4
- Zhou, X.; Wang, D.; and Krähenbühl, P. 2019. Objects as points. *arXiv preprint arXiv:1904.07850*.
- Zhou, Y.; Zhu, Y.; Ye, Q.; Qiu, Q.; and Jiao, J. 2018. Weakly supervised instance segmentation using class peak response. In *Proceedings of the IEEE Conference on Computer Vision and Pattern Recognition*, 3791–3800. 1, 2, 4
- Zhu, Y.; Zhou, Y.; Xu, H.; Ye, Q.; Doermann, D.; and Jiao, J. 2019. Learning instance activation maps for weakly supervised instance segmentation. In *Proceedings of the IEEE Conference on Computer Vision and Pattern Recognition*, 3116–3125. 2, 7

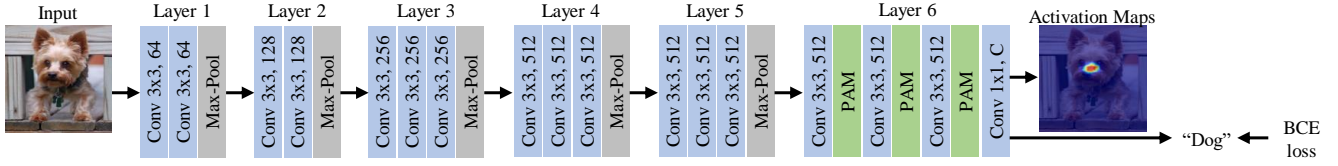


Figure 9: The detailed architecture of our classification network. BCE loss means the binary cross entropy loss function. The PAM is equipped in last three convolutional layers and trained with a self-supervised scheme.

## Appendix: Details of Peak Attention Module (PAM)

### Implementation Details

As described in the main paper, we extract instance cues from the classifier with our PAM. Here, we explain the implementation details of the PAM. We employ VGG-16 (Simonyan and Zisserman 2014) classifier and plugin our PAM into the last three convolutional layers of the classifier. The architecture of the classifier with PAM is illustrated in Figure 9. For training the classifier with PAM, we use the binary cross-entropy loss function and the stochastic gradient descent (SGD) optimizer with a weight decay of 0.0005 and a momentum of 0.9. The initial learning rate is set to 0.001 and is decreased by a factor of 10 at epoch 5 and 10. For data augmentation, images are randomly cropped to  $321 \times 321$ , and random horizontal flipping and random color jittering are applied. We use a batch size of 5 and train the classifier for 15 epochs. In the following section, we analyze how the PAM module affects each layer.

### Effect of PAM on each layer of Classifier

In this section, we analyze the effect of the PAM on each layer of the classifier. With the classifier described in Figure 9 as our baseline, we plug-in or plug-out the module. For the quantitative comparison as in Table 4, we evaluate the mean average precision (mAP) of our instance segmentation network without the Mask R-CNN refinement step. Since our PAM strengthens the attention on peak regions by deactivating noisy regions, we necessary to accurately distinguish between peak and noise regions. In lower-level layers (*i.e.*, layer-1, layer-2, and layer-3), the classifier captures the local features such as edges, and the definition of the peak region is unclear, so the effect of the PAM is minor. In contrast, in higher-level layers (*i.e.*, layer-4, layer-5, and layer-6), especially in the last layer, the classifier captures the global features, and the distinction between peak regions and noisy regions is more clear; our PAM plays a meaningful role in the last layer. From the results in Table 4, we note that the PAM equipped in only the last layer yields the best performance (41.1%  $mAP_{50}$ ) but the PAM equipped in the last three layers significantly degrades the performance (34.0%  $mAP_{50}$ ). We conclude that it is most effective to use the PAM only in the last layer where the definition of peak regions and noisy regions is the most obvious, and excessive modulization of PAM might deactivate the important features, degrading the performance.

Table 4: Effect of the PAM on each layer of the classifier.  $\checkmark$  means the PAM is equipped.

layer4	PAM layer5	layer6	$mAP_{25}$	$mAP_{50}$	$mAP_{75}$
		$\checkmark$	40.8	34.0	19.2
	$\checkmark$	$\checkmark$	<b>54.0</b>	<b>41.1</b>	<b>23.6</b>
$\checkmark$	$\checkmark$	$\checkmark$	50.0	38.7	23.4
$\checkmark$		$\checkmark$	44.1	34.0	20.6
$\checkmark$			53.0	39.2	23.2
$\checkmark$			48.8	36.8	21.4
	$\checkmark$		50.3	38.9	22.7
$\checkmark$	$\checkmark$		49.9	37.9	22.2

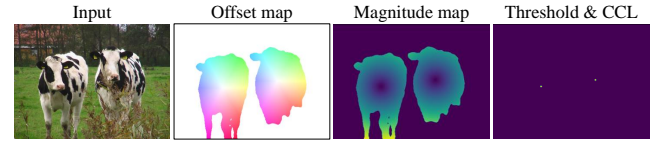


Figure 10: Illustration of the center clustering algorithm. The blue and yellow pixels in the magnitude map indicate that pixel values are close to zero and far from zero, respectively.

## Appendix: Detail of Center Clustering Algorithm

For the complementary knowledge between each network output, we employ the center clustering algorithm to extract center points from the offset map when generating the refined label. Here, we describe a detailed algorithm for the center clustering with a Figure 10. First, from the offset map, we create a magnitude map where each pixel represents the magnitude of the 2D vector. In this magnitude map, the pixel near the center of each instance is close to zero. Second, we apply a threshold to the magnitude map. We set the threshold to 2.5. Last, we extract the center point of each mask candidate obtained from the connected component labeling (CCL) algorithm. Here, we observe that the optimal area of the mask candidate is determined according to the threshold. For example, when the threshold is 2.5, the desired area of the mask candidate is near 21. For reliability-check utilizing the above observation, we additionally check whether the area of the mask candidate is between  $21 - \epsilon$  and  $21 + \epsilon$ ; we empirically set the  $\epsilon$  to 3. Due to this reliability-check process, we can prevent extracting false center points from the unstable offset map in the early training stage.

Table 5: Comparison of weakly-supervised instance segmentation methods on the Pascal VOC 2012 validation set. All methods adopt the Mask R-CNN instance segmentation network. We denote supervision sources as:  $\mathcal{F}$  (full mask),  $\mathcal{P}$  (point),  $\mathcal{C}$  (object count),  $\mathcal{B}$  (bounding box). We indicate the annotation cost per image in seconds for each supervision source. The  $\mathcal{M}$  means the segment proposal method (MCG) is employed.  $\dagger$  means that CRF (Krähenbühl and Koltun 2011) post-processing is utilized.

Method	Sup	Extra	$mAP_{25}$	$mAP_{50}$	$mAP_{70}$	$mAP_{75}$	Cost
Mask R-CNN (He et al. 2017)	$\mathcal{F}$	-	76.7	67.9	52.5	44.9	239.7
OCIS (Cholakkal et al. 2019)	$\mathcal{C}$	$\mathcal{M}$	48.5	30.2	-	14.4	22.2
WISE-Net (Laradji et al. 2020)	$\mathcal{P}$	$\mathcal{M}$	53.5	43.0	-	25.9	23.3
SDI (Khoreva et al. 2017)	$\mathcal{B}$	$\mathcal{M}$	-	44.8	17.8	-	38.1
BBTP (Hsu et al. 2019)	$\mathcal{B}$	-	74.0	54.1	24.5	17.1	38.1
BBTP $\dagger$ (Hsu et al. 2019)	$\mathcal{B}$	-	75.0	58.9	30.4	21.6	38.1
Arun et al. (Arun, Jawahar, and Kumar 2020)	$\mathcal{B}$	$\mathcal{M}$	73.1	57.7	33.5	31.2	38.1
BoxInst (Tian et al. 2021)	$\mathcal{B}$	-	-	61.4	-	37.0	38.1
BBAM (Lee et al. 2021a)	$\mathcal{B}$	-	-	61.9	-	25.8	38.1
BBAM (Lee et al. 2021a)	$\mathcal{B}$	$\mathcal{M}$	76.8	63.7	39.5	31.8	38.1
ours	$\mathcal{P}$	-	66.2	56.0	36.5	29.5	23.3

## Appendix: Additional Analysis

### Does iterative training help?

Most existing weakly-supervised learning methods maximize their performance by adopting the multi-step iterative training strategy; they iteratively generate pseudo labels from the network when training is complete and then re-train the network using the pseudo labels in offline manner. This strategy gives a progressive improvement but requires a huge training complexity. Our *self-refinement* plays a similar role with the iterative training but refines the pseudo labels in an online manner, requiring only a single-step training procedure. Here, we conduct an experiment to confirm that our single-step *self-refinement* is enough. When we adopt the two-step iterative training, we can obtain only 0.1% improvement. The three-step iterative training does not give any improvement compared to the two-step. This result demonstrates that our *self-refinement* is a quite efficient refinement method.

### Point-Supervised Instance Segmentation

In this section, we re-emphasize that the point label can be effectively exploited for WSIS. Seminar works (Bearman et al. 2016; Bellver Bueno et al. 2019) define the annotation cost of each supervision source: image-level (20.0 sec /img), object count (22.22 sec /img), point (23.3 sec /img), bounding box (38.1 sec /img), and full mask (239.7 sec /img). Compared to the image-level label, the point label contains the instance presence cue and is a budget-friendly label, requiring 16.5% more cost. The bounding box contains the exact region of interest for each instance, and now the matter is how to obtain a precise instance mask within the instance region. The box-supervised instance segmentation makes the WSIS easier task, however, the annotation cost is expensive, requiring 90.5% more cost than the image-level label and 63.5% more cost than point label. Nevertheless, as in Table 5, our point-supervised approach achieves quite competitive performance to other box-supervised approaches; compared to our approach, the current state-of-the-art box-supervised method without the off-the-shelf proposals requires 63.5% more annotation cost but achieves

10.5% higher performance. This result demonstrates that our well-designed approach can make excellent use of point labels for effective WSIS.

### Ablation Study for Hyperparameters

Here, we analyze some hyperparameters we used. First is  $\delta_p$  that is a threshold for extracting instance cues from PAM and is set to 0.5. When we change the  $\delta_p$  to 0.3 and 0.7, the number of true-positives in pseudo labels changes slightly, but the  $mAP_{50}$  variation is quite small to  $\pm 0.1\%$ . This is because our *self-refinement* method can progressively refine the pseudo labels and increase the number of true-positives.

Second is a threshold for the output center map. When generating refined labels, we perform the instance grouping algorithm using center points extracted from the output center map. Here, we extract the center point whose value is larger than  $\delta_c$ , which is set to 0.1. When we change the  $\delta_c$  to 0.3,  $mAP_{50}$  is almost maintained due to our soft labeling strategy using the weight mask  $\mathcal{M}$ .

Third is  $\lambda$  that is a weight parameter for our final objective function:  $\lambda_{center}$  for the center map,  $\lambda_{offset}$  for the offset map, and  $\lambda_{seg}$  for the semantic segmentation map. Since we adopt the instance segmentation network from Panoptic-DeepLab (Cheng et al. 2020), we follow their hyperparameter setting,  $\lambda_{center} = 200$ ,  $\lambda_{offset} = 0.01$ , and  $\lambda_{seg} = 1$ . And, we empirically find that changing  $\lambda_{seg}$  to 20 yields a 0.7%  $mAP_{50}$  improvement.

Last is the class-wise center map. As mentioned in the experiment section, we modify the original Panoptic-DeepLab network; we change the class-agnostic center map to the class-wise center map. This modification yields a 1.0%  $mAP_{50}$  improvement due to more accurate instance grouping; compared to the full supervision, our noisy offset vectors in the offset map are sometimes grouped with incorrect center points. To prevent incorrect instance grouping, we restrict the centers of other classes not to be grouped by adopting the class-wise center map.



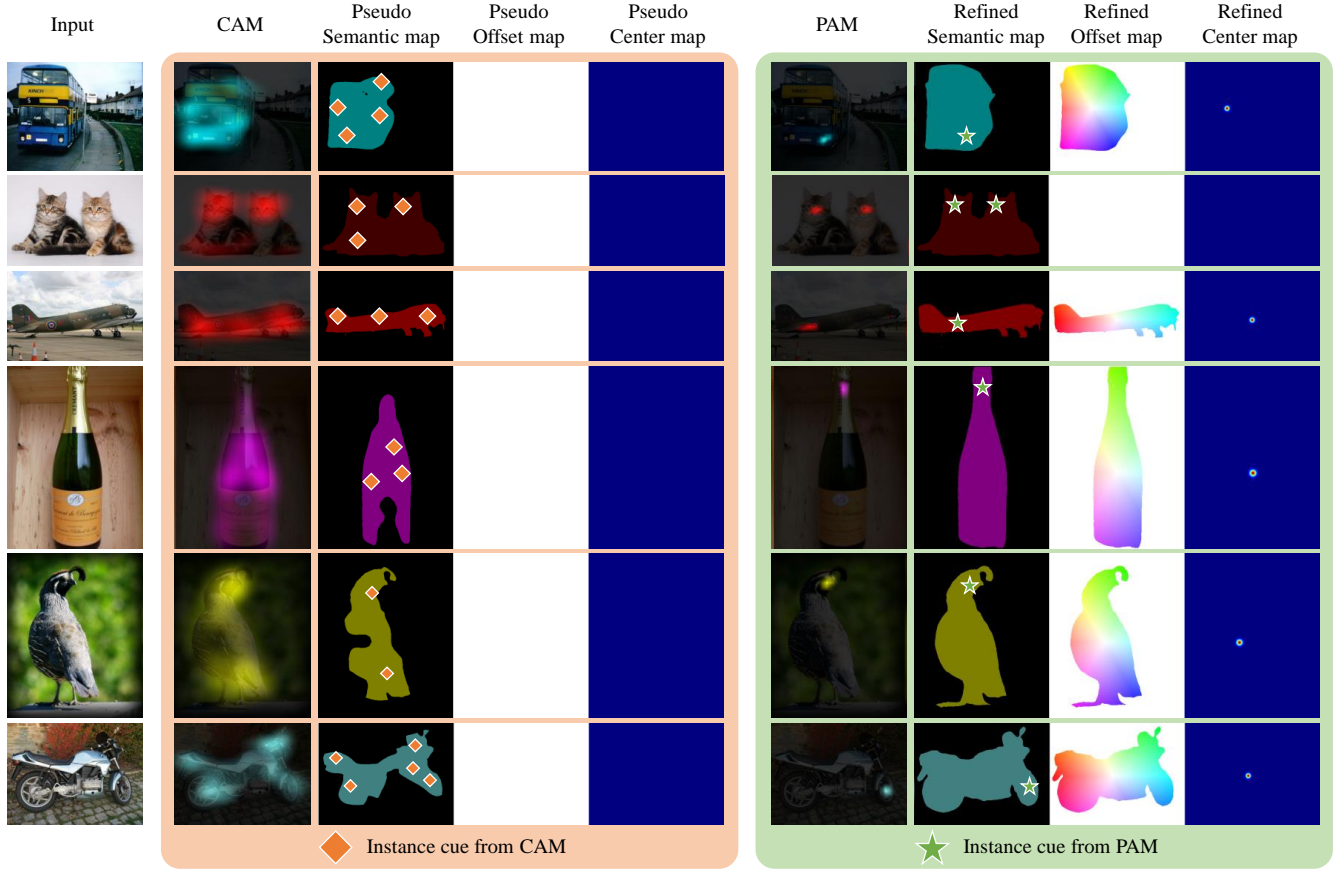


Figure 11: Qualitative results of initial labels generated from conventional CAMs (orange region) and initial labels generated from our PAM (green region). PAM can extract one peak point per instance.

## Appendix: Qualitative Results of Pseudo Label

In Figure 11, we provide more qualitative results of activation maps and pseudo labels. As in the orange area of Figure 11, the conventional CAMs have a limitation in generating high-quality pseudo labels due to the noisy activation region. However, as in the green area of Figure 11, our PAM produces sparse CAMs that help to extract one instance cue per instance. Therefore, from the *semantic knowledge transfer*, we can obtain more reliable pseudo labels, and the pseudo labels contain more true positive training samples.

## Appendix: Qualitative Results of Network outputs

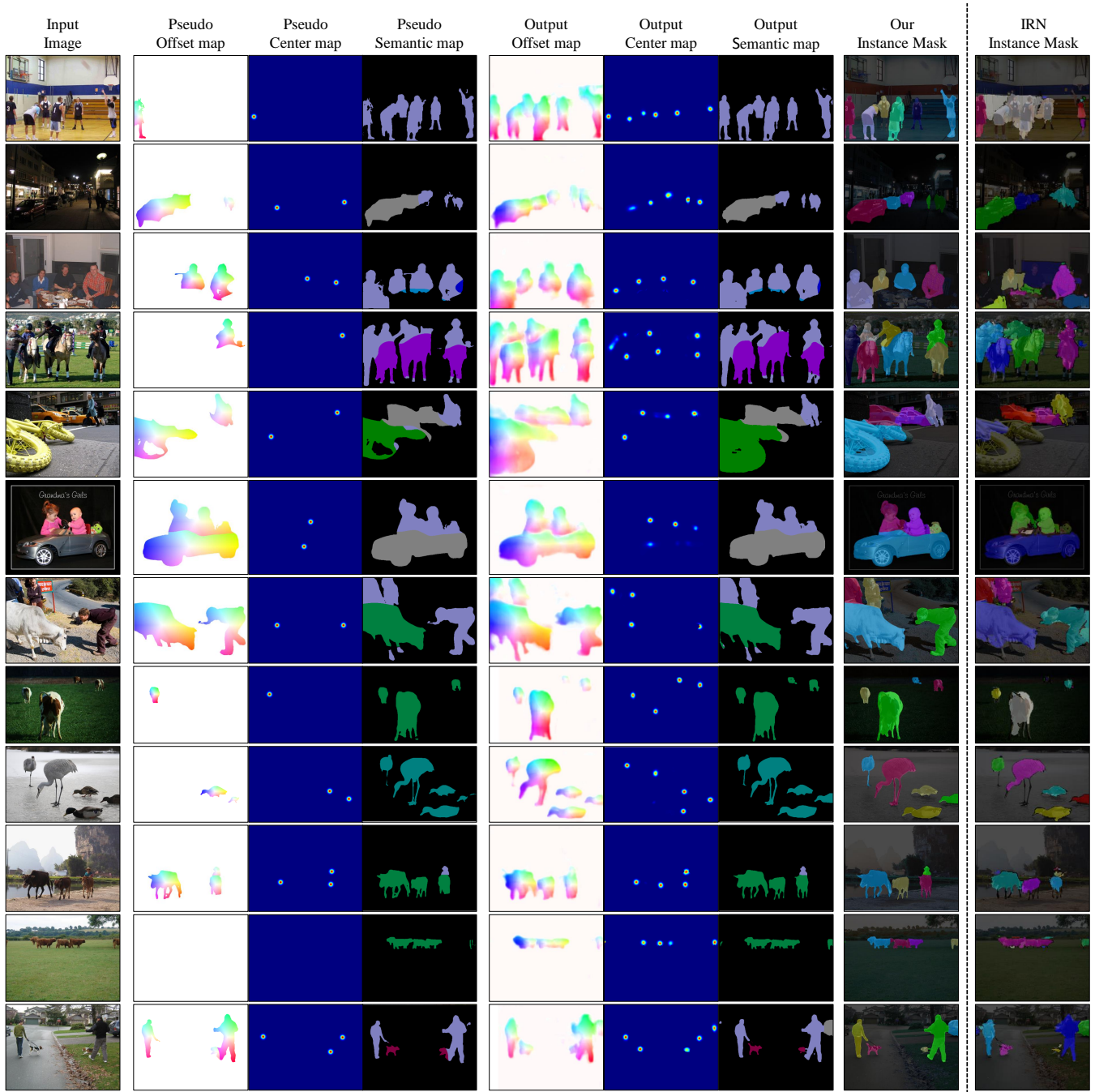
In Figure 12, we provide more qualitative results of our pseudo labels and network outputs. The pseudo label provides some reliable true-positive samples but contains lots of false-negatives (*i.e.*, unlabeled instances). Due to the proposed *self-refinement* with the *instance-aware guidance*, the network can produce high-quality instance masks including missing instances in pseudo labels. In addition, we compare our instance mask with that of IRN (Ahn, Cho, and Kwak 2019), which is the proposal-free method. The comparison results clearly show that our approach can properly segment multiple instances with a high-precision instance mask.

## Appendix: Failure Cases for PAM

We provide some failure cases of PAM in Figure 13, and these examples demonstrate the superiority of the point-supervised setting because inaccurate instance cues are replaced by ground-truth points. PAM has trouble in accurately localizing overlapping instances, which leads to the incorrect pseudo label (first row in Figure 13). In addition, missing instance cue or noisy localization increases missing instances in the pseudo label (second and third rows in Figure 13). Last, the WSSS method is trained with only image-level labels, some insufficient semantic segmentation maps yield inaccurate pseudo labels (last row in Figure 13).

## Appendix: Failure Cases for Proposed Method

We provide some failure cases of our WSIS method in Figure 14. First, when center points of instances are close to each other, we often fail to obtain the proper instance masks (first row in Figure 14); however, the keypoint-based method has suffered this issue even in a fully-supervised setting. In addition, noisy center and offset maps lead to false instance masks (second and third rows in Figure 14). Last, when the semantic segmentation map provides a noisy foreground region, we often fail to obtain the precise instance mask.



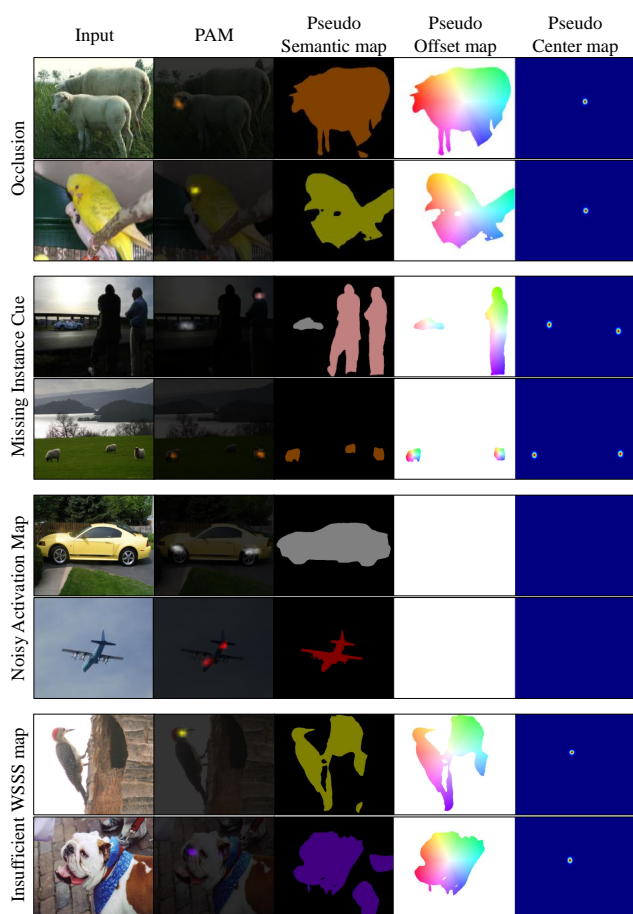


Figure 13: Failure cases of the PAM.

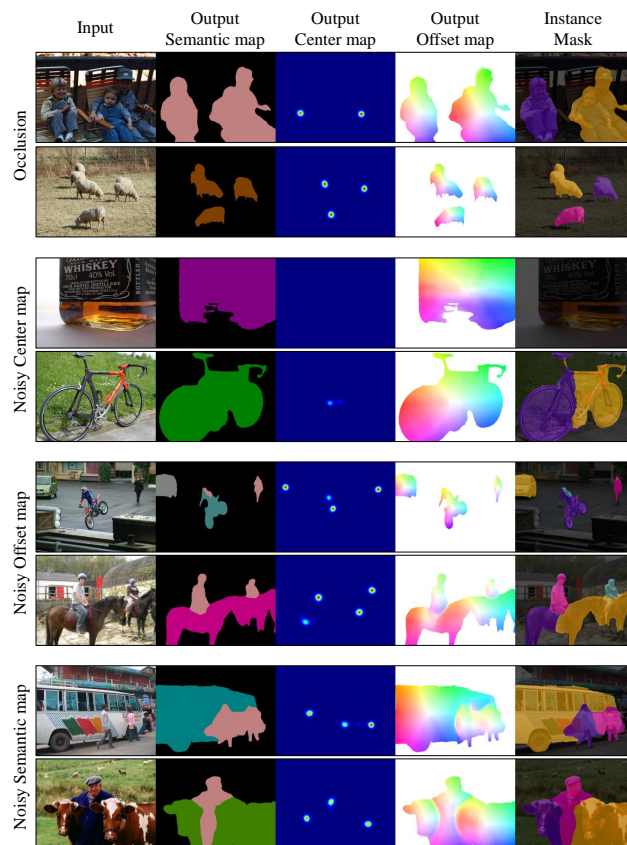


Figure 14: Failure cases of the proposed method.